Stem Cell Reports, Volume *13*

Supplemental Information

*PSEN1*ΔE9, *APPswe*, and *APOE4* Confer Disparate Phenotypes in Human iPSC-Derived Microglia

Henna Konttinen, Mauricio e Castro Cabral-da-Silva, Sohvi Ohtonen, Sara Wojciechowski, Anastasia Shakirzyanova, Simone Caligola, Rosalba Giugno, Yevheniia Ishchenko, Damián Hernández, Mohammad Feroze Fazaludeen, Shaila Eamen, Mireia Gómez Budia, Ilkka Fagerlund, Flavia Scoyni, Paula Korhonen, Nadine Huber, Annakaisa Haapasalo, Alex W. Hewitt, James Vickers, Grady C. Smith, Minna Oksanen, Caroline Graff, Katja M. Kanninen, Sarka Lehtonen, Nicholas Propson, Michael P. Schwartz, Alice Pébay, Jari Koistinaho, Lezanne Ooi, and Tarja Malm

Supplemental Figures

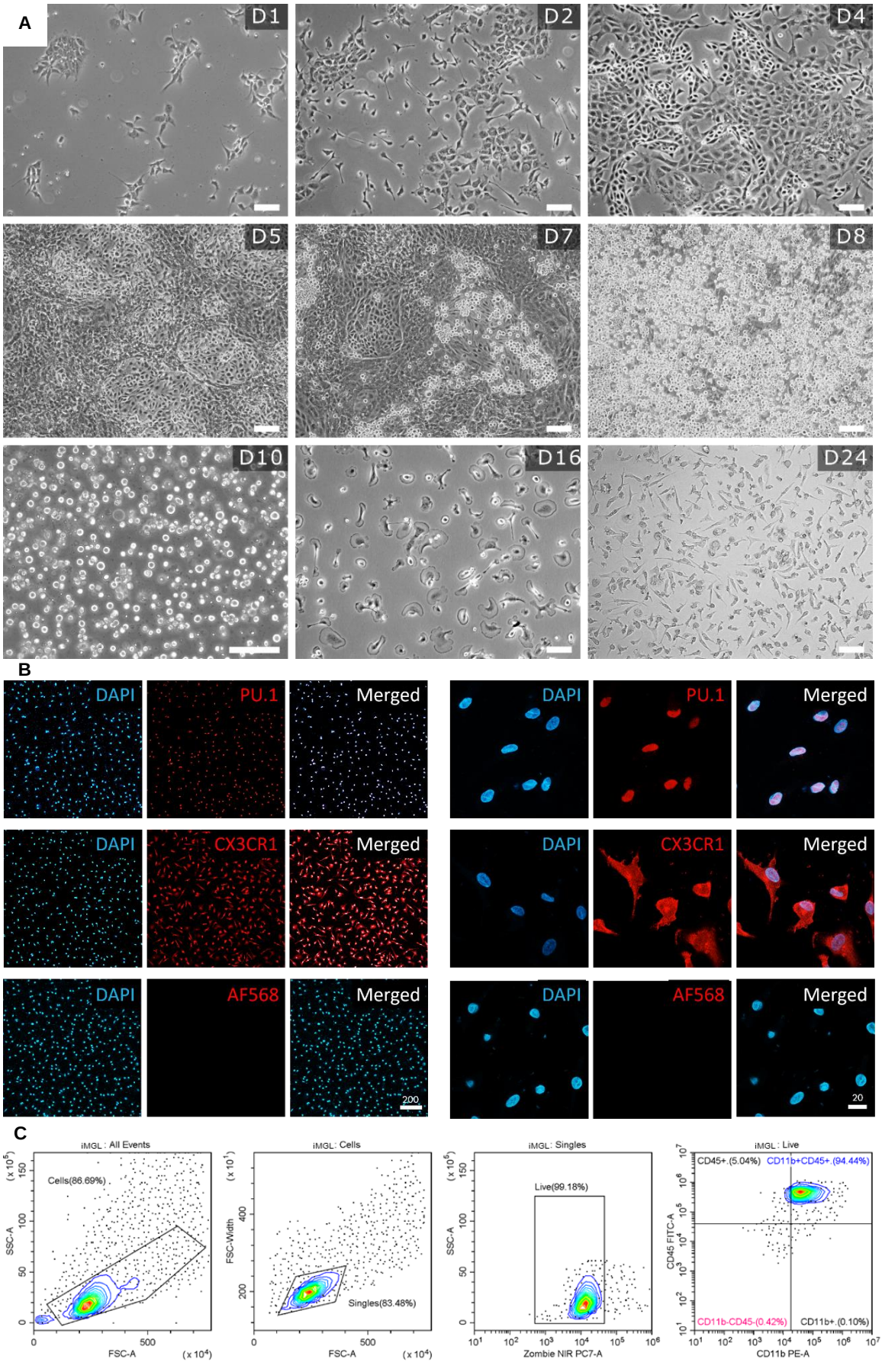

Figure S1. Microglial identity of iMGLs. Related to Figure 1.
(A) Morphological changes during iMGL differentiation presented as bright field images taken using ZEISS IX70 microscope with Axio Observer.Z1 (ZEISS) with 5X magnification. D1-D8 present images from Matrigel dishes, D10 and D16 on ULA-dishes and D24 shows the cells on PDL-coating. When the cells were maintained on ULA dishes after D16, they continued to have lamellipodia as presented in D16 image, whereas on PDL-coated vessels, the cells adopted more ramified and elongated morphology as presented on D24 image. Scale bar 100 µm. **(B)** Representative immunocytochemistry images of D24 iMGLs labeled with DAPI (blue) and PU.1 (red), CX3CR1 (red), or only with secondary antibody AF568 as a negative control with no primary antibody. Scale bar µm. **(C)** Representative gating strategy for flow analysis for CD11b-PE and CD45-FITC double stained D24 iMGLs.

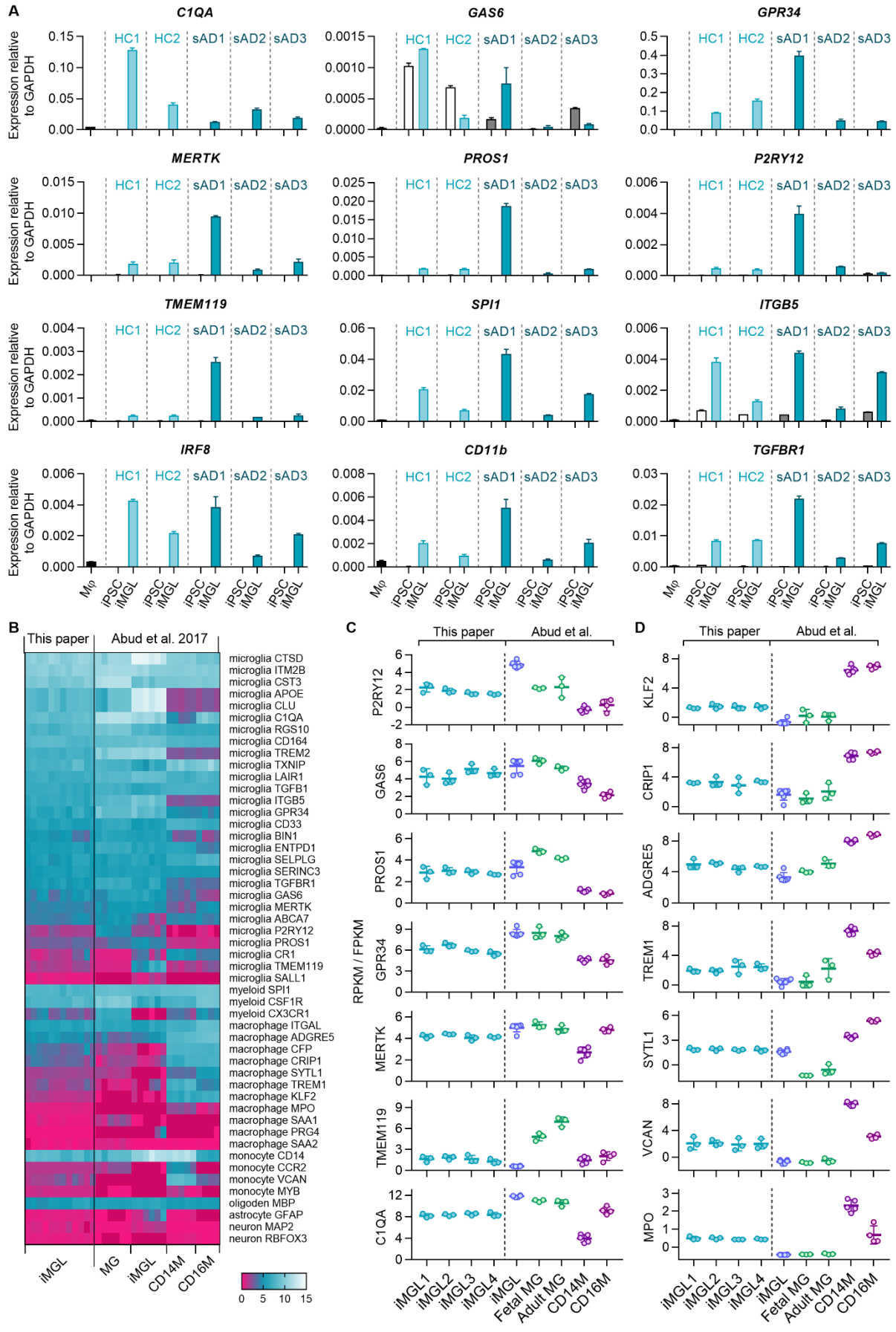
A
C1QA
GAS6
GPR34
MERTK
PROS1
P2RY12
TMEM119
SPI1
ITGB5
IRF8
CD11b
TGFBR1
Expression relative to GAPDH
HC1
HC2
sAD1
sAD2
sAD3
Mφ
iPSC
iMGL
B
This paper
Abud et al. 2017
microglia CTSD
microglia ITM2B
microglia CST3
microglia APOE
microglia CLU
microglia C1QA
microglia RGS10
microglia CD164
microglia TREM2
microglia TXNIP
microglia LAIR1
microglia TGFB1
microglia ITGB5
microglia GPR34
microglia CD33
microglia BIN1
microglia ENTPD1
microglia SELPLG
microglia SERINC3
microglia TGFBR1
microglia GAS6
microglia MERTK
microglia ABCA7
microglia P2RY12
microglia PROS1
microglia CR1
microglia TMEM119
microglia SALL1
myeloid SPI1
myeloid CSF1R
myeloid CX3CR1
macrophage ITGAL
macrophage ADGRE5
macrophage CFP
macrophage CRIP1
macrophage SYTL1
macrophage TREM1
macrophage KLF2
macrophage MPO
macrophage SAA1
macrophage PRG4
macrophage SAA2
monocyte CD14
monocyte CCR2
monocyte VCAN
monocyte MYB
oligoden MBP
astrocyte GFAP
neuron MAP2
neuron RBFOX3
iMGL
MG
iMGL
CD14M
CD16M
0 5 10 15
C
This paper
Abud et al.
RPKM / FPKM
P2RY12
GAS6
PROS1
GPR34
MERTK
TMEM119
C1QA
iMGL1
iMGL2
iMGL3
iMGL4
iMGL
Fetal MG
Adult MG
CD14M
CD16M
D
This paper
Abud et al.
KLF2
CRIP1
ADGRE5
TREM1
SYTL1
VCAN
MPO
iMGL1
iMGL2
iMGL3
iMGL4
iMGL
Fetal MG
Adult MG
CD14M
CD16M

Figure S2. Microglial gene expression. Related to Figure 1.
qRT-PCR and RNA-seq verifies that iMGL represent microglia-like gene expression and transcriptomic profile and cluster together with human microglia. **(A)** The qRT-PCR of 12 microglial signature genes was analyzed relative to GAPDH from RNA harvested from iPSCs and iMGLs as well as from human PBMC-derived CD14+ macrophages (Mφ). Representative data from two healthy control (HC) and three symptomatic LOAD (sAD) lines shown. n=3 technical replicates, repeated in three experiments. **(B)** Heat map of the RPKM/FPKM values from RNAseq data show that multiple microglial genes are highly expressed whereas macrophage genes are expressed at lower levels in iMGLs of this paper and (Abud et al., 2017) iMGLs and primary microglia (MG) compared to CD14M and CD16M monocytes/macrophages. ISO, isogenic. n=12 iMGLs including 4 cell lines from 3 batches. For further details, see Supplemental Experimental Procedures. (C) Corresponding bar figures for RPKM/FPKM values of microglial signature genes. (D) Corresponding bar figures for macrophage genes.

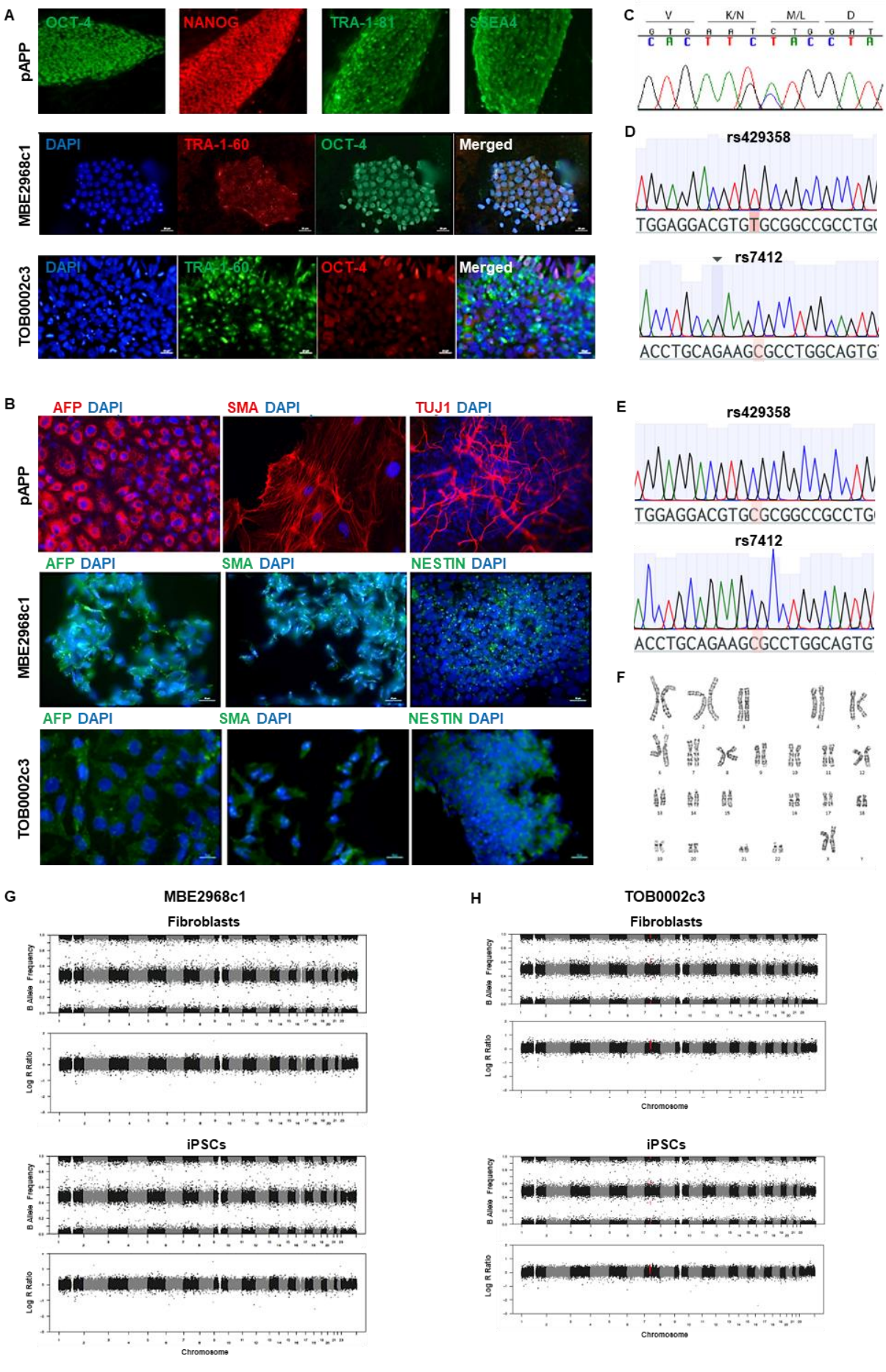
A
pAPP
OCT-4
NANOG
TRA-1-81
SSEA4
MBE2968c1
DAPI
TRA-1-60
OCT-4
Merged
TOB0002c3
DAPI
TRA-1-60
OCT-4
Merged
B
AFP DAPI
SMA DAPI
TUJ1 DAPI
pAPP
AFP DAPI
SMA DAPI
NESTIN DAPI
MBE2968c1
AFP DAPI
SMA DAPI
NESTIN DAPI
TOB0002c3
C
V
K/N
M/L
D
D
rs429358
TGGAGGACGTGTGCGGCCGCCTG
rs7412
ACCTGCAGAAGCGCCTGGCAGTG
E
rs429358
TGGAGGACGTGCGCGGCCGCCTG
rs7412
ACCTGCAGAAGCGCCTGGCAGTG
F
G
MBE2968c1
Fibroblasts
B Allele Frequency
Log R Ratio
iPSCs
B Allele Frequency
Log R Ratio
Chromosome
H
TOB0002c3
Fibroblasts
B Allele Frequency
Log R Ratio
Chromosome
iPSCs
B Allele Frequency
Log R Ratio
Chromosome

Figure S3. Characterization of pluripotency of pAPP, MBE2968c1 and TOB0002c iPSC cell lines. Related to Figure 2.

(A) Representative images of showing expression of the pluripotency markers TRA-1-81, NANOG, SSEA4TRA-1-60 or OCT4. **(B)** Representative germ layer immunostaining for clones differentiated to endoderm (AFP), mesoderm (SMA) and ectoderm (TUJ1 or NESTIN). Genomic Sanger sequencing of **(C)** pAPP showing a double mutation *APP KM670/671NL* (Swedish) at rs63751263 and rs63750445. Sanger sequencing for *APOE* at rs429358 and rs7412 loci confirming **(D)** *APOE3/3* status of MBE2968c1 and **(E)** *APOE4/4* status of TOB0002c3. **(F)** Karyotype of pAPP iPSCs. Copy Number Variation Analysis of the original fibroblasts and iPSCs (p8) for **(G)** MBE2968c1 and **(H)** TOB0002c3. Each panel shows the B allele frequency (BAF) and the log R ratio (LRR). BAF at values others then 0, 0.5 or 1 indicate an abnormal copy number. Similarly, the LRR represents a logged ratio of "observed probe intensity to expected intensity". A deviation from zero corresponds to a change in copy number. See also Table S3.

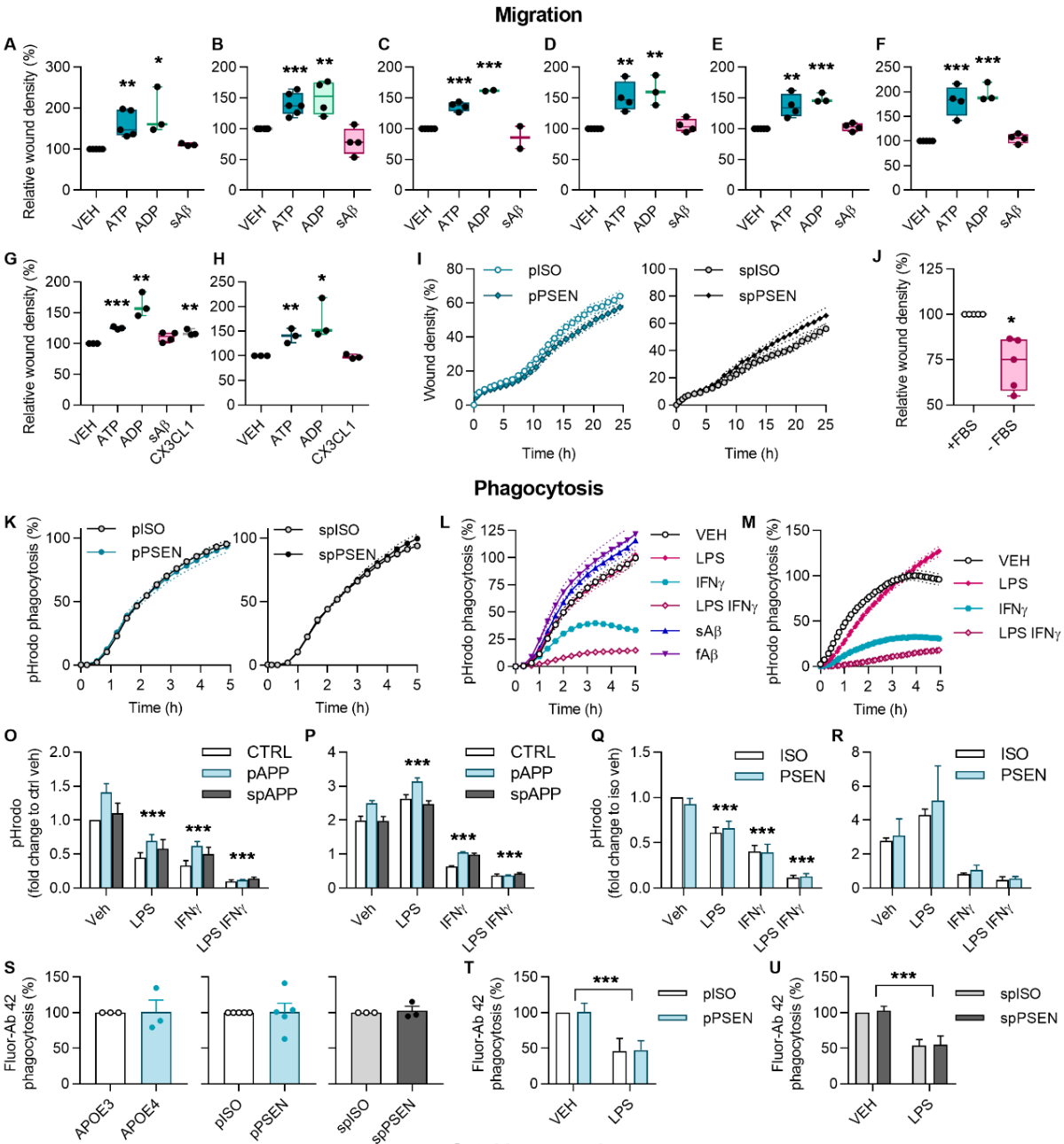
Migration
A
B
C
D
E
F
Relative wound density (%)
VEH
ATP
ADP
sAβ
G
H
CX3CL1
I
pISO
pPSEN
spISO
spPSEN
Wound density (%)
Time (h)
J
+FBS
-FBS
Phagocytosis
K
L
M
pHrodo phagocytosis (%)
VEH
LPS
IFNγ
LPS IFNγ
sAβ
fAβ
O
P
Q
R
pHrodo
(fold change to ctrl veh)
CTRL
pAPP
spAPP
Veh
(fold change to iso veh)
ISO
PSEN
S
T
U
Fluor-Ab 42
phagocytosis (%)
APOE3
APOE4
Cytokine secretion
V
W
X
Y
LPS-induced cytokine
(fold change)
IFNγ-induced cytokine
IL-6
TNFα
MCP1
RANTES
IL-8

Figure S4. Scratch wound migration, phagocytosis and cytokine secretion. Related to Figures 4-6.
Quantification of relative wound density in response to 100 µM ADP, ATP or fractalkine (CX3CL1) and 1 µM sAβ treatments normalized to vehicle (VEH). **(A)** healthy control, **(B)** pre-symptomatic *APPswe* **(C)** symptomatic *APPswe*, **(D))** isogenic control of symptomatic *PSEN1ΔE9*, **(E)** symptomatic *PSEN1ΔE9*, **(F)** pre-symptomatic *PSEN1ΔE9*, **(G)** *APOE3*, and for **(H)** *APOE4* iMGLs (n=2-6 batches, each with 4-5 wells). **(I)** Representative curves for wound density show no differences between *PSEN1ΔE9* and isogenic control iMGLs. n=4 wells. **(K)** Withdrawal of FBS (-FBS) reduced migration for 27% compared to normal medium (+FBS) at 25h. n=5 batches, each with 4-5 wells. **(K)** Representative curves for Zymosan A pHrodo phagocytosis in pre-symptomatic and symptomatic *PSEN1ΔE9* iMGLs and their isogenic controls. **(L)** Representative curves for pHrodo phagocytosis in control iMGLs with 24h pretreatment with 100 ng/ml LPS, 20 ng/ml IFNγ, 1 µM sAβ and 1 µM fAβ. **(M)** Corresponding representative curves when stimuli is withdrawn just before the measurements. Fold change in compared to control vehicle group after **(O)** 2 h (n=4 batches) and **(P)** 6 h (n=3 batches) depicting time-dependent response in vehicle and LPS groups. Respective graphs for isogenic and *PSEN1ΔE9* iMGLs at **(Q)** 2h (n=8 batches) and **(R)** 6h (n=2 batches). **(S)** Fluorescent Aβ phagocytosis after 5h incubation in isogenic, *PSEN1ΔE9*, *APOE3* and *APOE4* experiments. **(T,U)** LPS 100 ng/ml reduces phagocytosis of fluorescent Aβ after 5h in both *PSEN1ΔE9* iMGLs and their isogenic controls. **(V)** *APPswe* iMGLs secreted less IL-6 and TNFα compared to control iMGLs after 24 h treatment with 100 ng/ml LPS, and **(W)** less IL-6 and RANTES compared to control iMGLs upon 20 ng/ml IFNγ (n=3-4 batches each with 4 wells). **(X)** *PSEN1ΔE9* iMGLs secreted less IL-6, TNFα, RANTES, and IL-8 after LPS treatment, and **(Y)** less RANTES after IFNγ treatment compared to their isogenic controls (n=4-7 batches, each with 4 wells). Data presented mean ± SEM unpaired two-tailed t-test, one-way ANOVA or two-way ANOVA followed by Bonferroni's post hoc test,*$p<0.05$, **$p<0.01$, ***$p<0.001$.

Supplemental Tables

Table S1. RPKM/FPKM values of genes of different cell types used to obtain the heatmap. Related to Figure S3. Included as a separate excel file.

Table S2. Signature of microglia genes used to perform hierarchical clustering. Related to Figure 1.

FUCA2	*SMAP2*	*TGFB1*	*ZBTB45*	*GOLM1*	*RPTOR*	*LEMD2*	*CXXC5*	*TMEM63A*
SYPL1	*ZMPSTE24*	*TMEM147*	*IRF2BPL*	*AKIRIN2*	*ZNF787*	*TAF6L*	*PIK3CD*	*TCF4*
IFFO1	*SCAMP1*	*ERF*	*SUPT7L*	*LMO2*	*RHOB*	*STX5*	*RGS19*	*PELI1*
EXTL3	*LPCAT2*	*HSPB1*	*YIPF4*	*CD63*	*SRPRB*	*FAM102B*	*BSG*	*GPAA1*
BID	*EDEM2*	*YKT6*	*ALG5*	*CD164*	*OSBPL11*	*IER5*	*STARD5*	*MAN1A2*
GLT8D1	*ERP29*	*TGFBR1*	*SLC35B1*	*GNS*	*MARCH1*	*PPP1R21*	*DCAKD*	*SLC29A3*
RNASET2	*CDIP1*	*ZFAND5*	*B4GALT4*	*EPC2*	*GTF2H2*	*TGFBR2*	*MZT2A*	*YTHDF2*
IFNΓR1	*CMTM6*	*TSPAN14*	*STAU1*	*BIN1*	*YIPF5*	*ABHD6*	*NRROS*	*PNP*
ATP6V0A1	*TMEM101*	*SYNGR2*	*SOX4*	*LRRC8A*	*SLC12A9*	*ZNF513*	*RHOG*	*SFT2D1*
MFAP3	*AGO1*	*TMEM104*	*TM9SF2*	*ST6GALNAC4*	*MFHAS1*	*DUSP7*	*FAM210A*	*UBE2J1*
AGA	*MFSD11*	*TNFAIP1*	*MBOAT7*	*DENND4C*	*TACC1*	*DAGLB*	*CD151*	*HACD2*
HSPA5	*MAST3*	*GAB1*	*FAM110A*	*CNPY3*	*MED22*	*GALNT10*	*MPI*	*ZNF580*
HEXB	*KCNK6*	*CD81*	*ERGIC3*	*FCHSD2*	*MSRB2*	*CAMLG*	*CTC1*	*SFT2D2*
HERPUD1	*RNF215*	*ELK3*	*IRF3*	*NUMA1*	*RGS10*	*PEX2*	*CALR*	*SIPA1*
GINM1	*MFNG*	*CNOT2*	*SLC10A3*	*RDX*	*PAK1*	*MID1IP1*	*ARID3B*	*DDAH2*
GDI2	*HPS4*	*LPCAT3*	*TMEM175*	*ADAM10*	*SOGA1*	*NDST2*	*ZBTB18*	*IRF9*
CASP8	*CCDC134*	*LDHB*	*YWHAH*	*ATRAID*	*PIP4K2A*	*TMEM135*	*LACC1*	*ALG3*
TMEM206	*SUN2*	*PRKAB1*	*ATF4*	*ATAD1*	*PDE3B*	*TSC22D4*	*FIZ1*	*DDX3X*
MEF2A	*PACSIN2*	*SERINC1*	*TPST2*	*ENTPD1*	*SCOC*	*MARS*	*MCFD2*	*PPP2R2A*
ERLEC1	*ALKBH1*	*SAYSD1*	*DNAJB9*	*ITGAV*	*FAM49B*	*PDIA3*	*NRIP1*	*TMEM185B*
SEL1L	*ARHGAP5*	*FBRSL1*	*SNX6*	*COPS4*	*CMTM7*	*TP53I13*	*ATP6AP2*	*TAPBP*
FAM3A	*ABHD12*	*RNF130*	*MAP1S*	*RAP1GDS1*	*SLFN13*	*NCKAP5L*	*TTC3*	*RDH14*
DERL2	*ADNP*	*ARSB*	*PPT1*	*BMP2K*	*PLCL2*	*NUDT16L1*	*PAQR7*	*GNG10*
ST6GAL1	*CTSZ*	*TTC1*	*MGAT1*	*CCNG2*	*CNOT8*	*TMUB2*	*SPATA13*	*IL10RB*
PICALM	*CST3*	*TXNDC15*	*NDFIP1*	*PAPSS1*	*MED7*	*MAT2A*	*PTTG1IP*	*TWF2*
HACD3	*RP2*	*KLHL18*	*IL13RA1*	*DUSP6*	*ST3GAL2*	*INPP5D*	*TM2D3*	*GATC*
SLC46A1	*CLN5*	*RTN4*	*STARD3*	*GIT2*	*SLC35B2*	*COMMD8*	*SNN*	*SRGAP2*
IL4R	*MGRN1*	*GGCX*	*CHSY1*	*CSAD*	*SPPL3*	*MAP2K1*	*BTBD6*	*STRADA*
ACER3	*N4BP1*	*GORASP2*	*SERPINF1*	*LPAR6*	*SKI*	*INO80E*	*ATP6V0A2*	*CYFIP1*
MKNK1	*SLC38A7*	*NFE2L2*	*PTPRA*	*RBM26*	*WASF2*	*PWWP2A*	*SP1*	*ORAI1*
REXO1	*USP10*	*TMEM59*	*SERINC3*	*TSPAN3*	*F11R*	*ZNF282*	*ZFP36L1*	
EPB41L2	*LMF1*	*SCAMP3*	*SARAF*	*SCAMP2*	*B4GALT3*	*ELP5*	*BICD2*	
STX7	*RAB11A*	*RGS2*	*CTIF*	*UNC45A*	*IFNΓR2*	*PFKFB3*	*TPCN1*	
SLC35C2	*BMF*	*ABCD3*	*VHL*	*ARMC5*	*ARHGAP27*	*KBTBD2*	*SEMA4D*	
SESN1	*LEPROTL1*	*RPS6KA1*	*ARL8B*	*PRPSAP2*	*BTG2*	*RNF139*	*PLSCR3*	
CLDND1	*ASAH1*	*CCNI*	*IL6ST*	*G6PC3*	*HK2*	*JAGN1*	*TSPYL1*	
RNF13	*CLPTM1*	*HS1BP3*	*TMED7*	*GALNT1*	*CCDC107*	*BCL2L1*	*PNRC2*	
OXCT1	*SNAPC2*	*NEK6*	*NAA35*	*SLC16A3*	*FMNL3*	*CLSTN1*	*SLC35E2B*	

Table S3. Demographic information of each iPSC-line. Related to Figure 2. See also Figure S3.

Alias	Cell line	Sex	Health status	Age at biopsy	Mutation genotype	Sample origin	Reprogramming method	Karyotype	Reference
CTRL	Ctrl1	F	Healthy	Adult	-	Skin biopsy	SeV 1.0	46XX Normal	Holmqvist et al. 2016
CTRL	Ctrl3	F	Healthy	44 y	-	Skin biopsy	SeV 1.0	46XX Normal	Oksanen et al. 2017
spPSEN	AD2	M	FAD	48 y	*PSEN1ΔE9* deletion	Skin biopsy	SeV 2.0	46XY Normal	Oksanen et al. 2017
pPSEN	AD3	F	FAD pre-symptomatic	47 y	*PSEN1ΔE9* deletion	Skin biopsy	SeV 2.0	46XX Normal	Oksanen et al. 2017
spISO	AD2 iso	M	FAD corrected	48 y	*PSEN1ΔE9* corrected	Skin biopsy	SeV 2.0 CRISPR/Cas9	46XY Normal	Oksanen et al. 2017
pISO	AD3 iso	F	FAD corrected	47 y	*PSEN1ΔE9* corrected	Skin biopsy	SeV 2.0 CRISPR/Cas9	46XX Normal	Oksanen et al. 2017
spAPP	LL008	F	FAD	48 y	*KM670/671NL* APP Swedish	Skin biopsy	SeV 1.0	46XX Normal	Oksanen et al. 2018
pAPP	LL116	F	FAD pre-symptomatic	30 y	*KM670/671NL* APP Swedish	Skin biopsy	SeV 2.0	46XX Normal	Figure S3.
APOE3	MBE 2968 clone 1	F	Healthy	65 y	*APOEε3/3*	Skin biopsy	Episomal reprogramming by nucleofection	46XX Normal	Figure S3.
APOE4	TOB 0002 clone 3	F	Non-symptomatic	52 y	*APOEε4/4*	Skin biopsy	Episomal reprogramming by nucleofection	46XX Normal	Figure S3.
APOE3	HC1	M	Healthy	57 y	*APOEε3/3*	Skin biopsy	mRNA	46XY Normal	Balez et al., 2016
APOE3	HC2	F	Healthy	75 y	*APOEε3/3*	Skin biopsy	mRNA	46XX Normal	Muñoz et al., 2018
APOE 3/4	HC3	F	Healthy	59 y	*APOEε3/4*	Skin biopsy	mRNA	46XX Normal	UOW - manuscript in preparation
APOE 3/4	LOAD1	M	LOAD	65 y	*APOEε3/4*	Skin biopsy	mRNA	46XY Normal	Balez et al., 2016
APOE4	LOAD2	F	LOAD	83 y	*APOEε4/4*	Skin biopsy	mRNA	46XX Normal	UOW - manuscript in preparation
APOE4	LOAD3	M	LOAD	77 y	*APOEε4/4*	Skin biopsy	mRNA	46XY Normal	Ooi et al., 2013

FAD, famimial Alzheimer's disease; LOAD, late-onset Alzheimer's disease; F, female; M, male; y, years.

Supplemental Experimental Procedures

Karyotyping

iPSCs were confirmed to have normal euploid karyotypes via Giemsa (G-banding) staining (pAPP) or by virtual karyotyping (TOB0002c3, MBE2968c1)(Figure S3). For Giemsa staining iPSCs were arrested with 200 ng/ml KaryoMAX® Colcemid™ (Invitrogen), harvested and 20 metaphase cells were analyzed at the Eastern Finland Laboratory Centre Joint Authority Enterprise (ISLAB, Kuopio, Finland). In virtual karyotyping the copy number variation (CNV) analysis of original fibroblasts and iPSCs was performed using HumanCore Beadchip arrays (Illumina). CNV analyses were performed using PennCNV and QuantiSNP (Wang et al., 2007, Colella et al., 2007) with default parameter settings. Chromosomal aberrations were deemed to involve at least 10 contiguous single nucleotide polymorphisms (SNPs) or a genomic region spanning at least 1MB. The B allele frequency (BAF) and the log R ratio (LRR) were extracted from GenomeStudio (Illumina) for representation. All three lines were confirmed to express high levels of pluripotent markers and to have the ability to form all three germ layers by immunocytochemistry. Embryoid bodies were obtained as described (Lim et al., 2013) and using tri-lineage differentiation kit (Stem Cell Technologies).

Flow Cytometer Analysis

The flow cytometer analysis was performed every second day throughout the 24-day differentiation process. Cells were detached with Accutase, centrifuged 300 x g, 5 min and filtered through a 70 µm mesh (Corning). Approximately 200 000 cells were used for each sample and staining controls, including unstained, single color, and secondary-only. Fluorescence minus one (FMO) controls were also prepared for gating purposes. Cells were stained with Zombie NIR fixable viability dye (1:1000, Biolegend), blocked with human FcR blocking reagent (Miltenyi Biotec), and then incubated with conjugated antibodies for 30 min at 4°C. The following antibodies were used: CD11b-APC-eFluor780 (M1/70), CD34-APC (4H11), CD41a-BB515 (HIP8), CD45-PerCP/Cy5.5 (2D1), CD117 (cKit)-BB515 (104D2), CD144 (VE-cadherin)-PE (55-7H1), CD235a (HIR2)-BB515 (GA-R2), and CD309 (KDR)-PE (89106). For intracellular staining, cells were fixed in Fix/Perm buffer for 25 min (Foxp3 Buffer Set, eBioscience), incubated with primary antibody IBA1 (1:50, Wako) for 40 min at 4°C, followed by labeling with secondary antibody goat anti-rabbit Alexa Fluor 488 (1:1000, Invitrogen) for 30 min at RT. Samples were washed between each step and resuspended in flow buffer containing 1% FBS in PBS. Samples were run on a FACSAriaIII (BD Biosciences), equipped with 488 and 633nm lasers with standard configuration or on CytoFlex S (Beckman Coulter) equipped with 405, 488, 561, and 638nm lasers. At least 50 000 single events were collected. Data was analyzed with FCSExpress v6 (De Novo) or CytExpert v2.3 (Beckman Coulter). The flow cytometry analysis was repeated with 4 cell lines including both AD and isogenic genotypes from 2-3 batches.

RNA-Seq and analysis

iMGLs were cultured at density of 2 mln cells per PDL-coated 6 cm dish and total RNA was extracted using mirVana™ miRNA Isolation Kit (Invitrogen) following manufacturer's guidelines. RNA integrity (RIN) was measured for all samples using the Bioanalyzer Agilent 2100 series. The quality was confirmed with Advanced Analytical Fragment Analyzer at Finnish Functional Genomics Centre (FFGC, Turku, Finland) and further library construction and sequencing was performed at FFGC. Total of 300 ng of high integrity RNA with RIN > 9.1 was used to generate sequencing libraries with Illumina TruSeq® Stranded mRNA to obtain poly-A mRNA. The high quality of the libraries was confirmed with Advanced Analytical Fragment Analyzer and the concentrations of the libraries were quantified with Qubit® Fluorometric Quantitation (Life Technologies). The samples were sequenced as single-end 50 bp reads on the Illumina HiSeq 3000 instrument.

Raw FASTQ files were analyzed for quality assessment using FastQC software. Read alignment and transcript quantification were performed using RSEM 1.3.1(Li, Dewey, 2011) with "--strandness reverse" and "--estimate-rspd" parameters. Hg38 was used as reference genome. All subsequent analyses were conducted with the R/Bioconductor platform. RSEM estimated counts were imported using the package Tximport (Soneson, Love & Robinson, 2015). This package allows to incorporate the average transcript length per gene as a normalization factor that can be used with statistical tools such as limma (Ritchie et al., 2015) and DESeq2 (Love, Huber & Anders, 2014). Hierarchical clustering was performed together with published data (Abud et al., 2017) using the function "hclust" with Euclidean distance on FPKM expression data. The analysis was performed using microglia signature genes (Table S2) adapted from already published data (Lavin et al., 2014) provided by the Bioconductor AUCell package (Aibar et al., 2017). Mouse identifiers have been mapped into HGNC symbols through the NCBI HomoloGene database (Wheeler et al., 2007). Genes with expression (< 1 FPKM) across all samples were discarded. Before clustering and other comparisons with data in Abud et al., the following preprocessing steps have been performed. The two studies have been separately log2-transformed (adding a pseudo-count of 1) and normalized for row using the function "normalize.quantiles" of the package preprocessCore that performs a normalization based on upon the concept of a quantile-quantile plot (Bolstad et al., 2003). Subsequently, data

have been batch corrected to remove the bias due to the technical variability of the two studies. Batch correction was performed using the function "removeBatchEffect" of the limma package.

qRT-PCR

The RNA was extracted from 10^6 *APOE* iMGLs, iPSCs and blood-derived macrophages using TRIsure reagent (Bioline) and genomic DNA was removed with TURBO DNA-free (Thermo Fisher Scientific) following the manufacturer's instructions. RNA concentration was analyzed using a Nanodrop 2000C spectrophotometer (Thermo Fisher Scientific). RNA was reverse transcribed to cDNA using the Tetro cDNA synthesis kit (Bioline) and Oligo dT18 primers incubated at 45 ^{o}C for 30 min followed by a 5 min incubation at 85 ^{o}C to terminate the reaction. Gene expression was measured by qRT-PCR using SENSIfast SYBR No-ROX PCR mix (Bioline) and a Rotor Gene 3000 Real-time PCR machine (Corbett Research) with 40 cycle amplification. Melt-curve analysis and gel electrophoresis were utilised to check amplicon size. Reactions were conducted in duplicate whilst non-template controls (substituting cDNA for water) and RNA controls were implemented to confirm that contamination, primer dimers and genomic DNA were not contributing to the signal. Data was normalised to GAPDH expression, sample efficiency/cycle threshold values were determined using LinRegPCR (Ruijter et al., 2009) and relative gene expression was determined by using the comparative threshold cycle method (Schmittgen, Livak, 2008). RNA was also extracted from *APPswe* and *PSEN1ΔE9* iMGLs and iPSCs by mirVana™ miRNA Isolation Kit (Invitrogen). Subsequent cDNA synthesis was performed with Maxima reverse transcriptase (Thermo Scientific) and the mRNA expression levels were determined by qRT-PCR (StepOne Plus Real-Time PCR system; Life Technologies) using TaqMan assay mixes (Thermo Scientific). Expression levels were normalized to *ACTB* and *GAPDG* expression.

Table of primers assay mixes used for mRNA expression studies.

Gene	**Identifier**	**Source**
ACTB	Hs99999903_m1	TaqMan
GAPDH	Hs02758991_g1	TaqMan
C1QA	Hs00706358_s1	TaqMan
C1qR	Hs00362607_m1	TaqMan
CD11b	Hs00355885_m1	TaqMan
P2RY12	Hs00224470_m1	TaqMan
CR1	Hs00559348_m1	TaqMan
CSF1R	Hs00911250_m1	TaqMan
PROS	Hs00165590_m1	TaqMan
GAS6	Hs01090305_m1	TaqMan
GPR34	Hs00271105_s1	TaqMan
MERTK	Hs01031979_m1	TaqMan
IRF8	Hs00175238_m1	TaqMan
PU.1	Hs02786711_m1	TaqMan
TREM2	Hs00219132_m1	TaqMan
TYROBP	Hs00182426_m1	TaqMan

Table of primers used for mRNA expression studies.

Target	Sequence	Species
hF_ITGAM-CD11B	GAAAGGCAAGGAAGCCGGAG	human
hR_ITGAM-CD11B	TGGATCTGTCCTTCTCTTAGCCG	human
hF_CX3CR1	TGGGGCCTTCACCATGGAT	human
hR_CX3CR1	GCCAATGGCAAAGATGACGGAG	human
hF_P2ry12	TTTGTGTGTCAAGTTACCTCCG	human
hR_P2ry12	CTGGTGGTCTTCTGGTAGCG	human
hF_IRF8	AGTAGCATGTATCCAGGACTGAT	human
hR_IRF8	CACAGCGTAACCTCGTCTTC	human
hF_MERTK	CTCTGGCGTAGAGCTATCACT	human
hR_MERTK	AGGCTGGGTTGGTGAAAA	human
hF_PROS1	TTGCACTTGTAAACCAGGTTGG	human
hR_PROS1	CAGGAACAGTGGTAACTTCCAG	human
hF_TGFBR1	ACGGCGTTACAGTGTTTCTG	human
hR_TGFBR1	GCACATACAAACGGCCTATCTC	human
hF_GAS6	CTCGTGCAGCCTATAAACCCT	human
hR_GAS6	TCCTCGTGTTCACTTTCACCG	human
hF_C1QA	TCTGCACTGTACCCGGCTA	human
hR_C1QA	CCCTGGTAAATGTGACCCTTTT	human
hF_GPR34	GCAAGGTTGTGGGAACACTGT	human
hR_GPR34	AGCGATCCAAACTGATGAATCC	human
hF_ITGB5	GGAAGTTCGGAAACAGAGGGT	human
hR_ITGB5	CTTTCGCCAGCCAAATCTTCTC	human
hF_CD14	ACTTATCGACCATGGAGCGC	human
hR_CD14	AGCTCACAAGGTTCTGGCGT	human
hF_TMEM119	CTTCCTGGATGGGATAGTGGAC	human
hR_TMEM119	GCACAGACGATGAACATCAGC	human
hF_SPI1	AGCCATAGCGACCATTAC	human
hR_SPI1	CTCCGTGAAGTTGTTCTC	human
hF_GAPDH	GAGCACAAGAGGAAGAGAGAGACCC	human
hR_GAPDH	GTTGAGCACAGGGTACTTTATTGATGGTACATG	human

Differentiation of human monocyte-derived macrophages from peripheral blood mononuclear cells

Human peripheral blood mononuclear cells (PBMCs) were isolated from the whole blood of anonymous donors (Australian Red Cross Blood Service, NSW) using Ficoll-Paque Plus (GE Healthcare) and density-gradient centrifugation. Briefly, whole blood was diluted 1:2 in phosphate buffered saline (PBS, layered above Ficoll and centrifuged for 45 min at 200 xg without deceleration. Following centrifugation, distinct phases were separated and the PBMC layer was collected and diluted 1:2 in PBS. Suspension was centrifuged at 500 x *g* for 10 min at 4°C. The pellet was washed three times with PBS by centrifugating 500 x *g* for 10 min at 4°C. Primary monocytes were isolated using magnetic microbead separation using CD14-conjugated microbeads under manufacturer specifications (Miltenyi Biotech) and positively selected cells were separated using LS+ columns (Miltenyi Biotec) positioned on a MidiMACS magnet (Miltenyi Biotec). Subsequent differentiation of CD14+ to macrophages was achieved by culturing the CD14+ cells in in high glucose DMEM, 10% FBS, 1% GlutaMAX, 1% P/S and 15 ng/ml MCSF (Miltenyi Biotec). The cells were seeded onto nunclon treated dishes at 10^6 cells/mL and incubated for 7 days at 37 ºC, 5% CO2. Differentiation was determined by observing cell morphology in a Nikon TS100 light microscope (Nikon).

3D co-cultures

3D thin-layer Matrigel cultures were prepared as previously described (Choi et al., 2014, Kim et al., 2015). iPSC-derived neurons were resuspended at $1x10^6$ cells/ml with 1:10 diluted Matrigel. plated on poly-L-ornithine-coated coverslips (Thermo Scientific) and left to polymerize overnight. On the next day, wells were filled with neural differentiation medium, consisting of DMEM/F-12 and Neurobasal (1:1), 1% B27 without vitamin A, 0.5% N2 supplement, 1% GlutaMAX™ and 0.5%P/S (all from Gibco), and the medium was changed every 3-4 days for 4-months. Then D16 iMGLs were applied on the top of cultures at density of 100,000 cells/ml. The 3D co-cultures were fixed and immunostained 7 days after incorporation of iMGLs.

3D cerebral brain organoids were generated as described (Lancaster, Knoblich, 2014). In brief, single iPSCs were seeded for embryoid body cultures in E8 with 20 µM Y-27632 on Nunclon Sphera 96-well plate. On D6, neuroinduction was initiated by replacing to 1:1 E8 and neuroinduction medium (NIM) composing of DMEM/F-12, 1% N2, 1% GlutaMAX, 1% of non-essential amino acid mixture (NEAA), 0.5% P/S (all from Gibco) and 5U/ml Heparin (LEO Pharma). On D11, the spheres were embedded into Matrigel droplets, and transferred into differentiation medium without vitamin A (Dif-A) composed of 1:1 DMEM/F-12 and Neurobasal, 1% GlutaMAX, 0.5% NEAA, 0.5% N2, 0.5% B27 without vitamin A, 0.5% P/S, 2.5 µg/ml insulin and 50 µM 2-mercaptoethanol (Sigma). On D15, the organoids were transferred to magnetic spinners (Corning) in Dif+A, which was otherwise identical to Dif-A, but B27 with vitamin A was used. For organoid and iMGLco-cultures, 200 0000 D16 iMGLs were transferred to 6-well ULA-plates with 10 organoids in Dif-A. After iMGLs freely attached to the organoids for 6 h, the organoids were transferred back to the magnetic spinners and were collected on D60 for immuhistochemical analysis.

Immunocytochemistry

The cell cultures were fixed in 4% paraformaldehyde (PFA), permeabilized in 0.5% Triton X-100 (Sigma) and 0.2% Tween20 or in 0.2% Tergitol-type NP-40 + 0.3 M glycine, and blocked with 10% normal goat serum (NGS). Primary antibodies were incubated overnight at 4°C followed by labelling with Alexa Fluor 488 (1:1000) and 568 (1:500) conjugated anti-rabbit secondary antibodies (Thermo Fisher Scientific) and nuclei were stained with 5 µg/ml Hoechst 33258 (Sigma) or 1 µg/mL Hoechst 33342 (Invitrogen). Reagents were prepared in tris-buffered saline that was used for washing between each step. 3D thin-layer Matrigel co-cultures were fixed and immunostained similarly but with longer incubation times as previously described (Kim et al., 2015, Choi et al., 2014). Coverslips were mounted on glass microscope slides using Prolong Gold Antifade reagent (Thermo Fisher Scientific) or mounting medium (Southern Biotech). Organoids were fixed with 4% PFA for 4 h followed by overnight incubation in 30% sucrose (VWR) at 4C and were then embedded into O.C.T. Compound (Sakura) for sectioning to 20 µm slices using Cryotome (Leica CM1950). Sections were transferred on microscope slides (Thermo Scientific), blocked in 10% NGS (Millipore) in 0.05% Tween20 (Sigma), incubated with a rabbit anti-Iba1 primary antibody overnight followed by secondary antibody Alexa fluor 568 goat anti-rabbit (1:500) labeling. Slides were mounted in Vectashield mounting medium with DAPI (Vector) for imaging. Staining cotrols that omitted the primary antibody or substituted it with an IgG isotype, were used to confirm staining specificity. Immunocytochemistry was visualized using a ZEISS LSM 800 Airyscan super resolution microscope (ZEISS) with 10x and 40x objectives, and 2 x GAsp and 1 x Airyscan detectors. Super resolution images were taken as z-stack images and were presented as maximum intensity projections. Images were exported using ZEN 2.3 software. Imaging conditions were kept constant across iMGLs and negative controls.

Table of primary antibodies used for immunocytochemistry.

Target	Dilution	Source	Catalog number
rabbit anti-Iba1	1:500	Wako	019-19741
rabbit anti-Iba1	1:500	Abcam	ab153696
rabbit anti-TMEM119	1:100	Abcam	ab185333
rabbit anti-CX3CR1	1:100	Abcam	ab8021
rabbit anti-TREM2	1:400	Cell Signaling Technology	91068
rabbit anti-PU.1	1:500	Cell Signaling Technology	2266
rabbit anti-P2RY12	1:125	Sigma	HPA014518

Western Blotting

Western blotting was done as described (Viswanathan et al., 2011) with minor changes. Two million iMGLs were lysed into T-PER tissue extraction buffer with a Halt™protease inhibitor and Halt™phosphatase inhibitor cocktails (all from Thermo Fisher Scientific). Protein concentrations were determined using Pierce™ BCA Protein Assay Kit (Thermo Fischer Scientific) and 15 µg proteins were separated on NuPAGE™ 4–12% Bis-Tris Midi gels (Invitrogen) under reducing conditions and blotted onto polyvinylidene difluoride membranes. The iBlot 2 PBDF Regular Stacks and Dry Blotting System (both from Invitrogen) were used to transfer the proteins. The membranes were probed with the anti-APP (1:2000, Sigma) and anti-PSEN1 (1:1000, Chemicon) to detect FL- and CTF-PSEN, and anti-GAPDH (1:15000, Abcam) antibodies and labeled with horseradish peroxidase (HRP)-conjugated mouse and rabbit secondary antibodies (GE Healthcare). Proteins were detected and visualized by using enhanced chemiluminescence substrate prime (GE Healthcare) and BioRad Chemi Doc™ imaging system. Images were quantified using Image Lab (Bio-Rad Laboratories, Inc.) and protein levels were normalized to GAPDH.

Aβ ELISA
The amounts of Aβ1-40 and Aβ1-42 were measured from 48 h conditioned cell culture medium and cell extract with Amyloid beta 40 and 42 Human ELISA Kits (Invitrogen). The cells were seeded on D16 on PDL-coated 24-well Nunc plates at final concentration of 250 000 cells/well and maintained normally until D24 before collecting the samples. Protease inhibitor cocktail (Sigma) with a serine protease inhibitor, was added 1:200 to samples. Conditioned medium from iPSC-derived neurons was used as positive control and the sample was prepared as described previously (Oksanen et al., 2017).

Ca^{2+} Imaging
iMGLs on PDL-coated coverslips were loaded with the calcium-sensitive fluorescent dye Fluo-4, AM (5 µM, Invitrogen) for 30 min followed by a 10-min washout in the basic solution containing 2.5 KCl (Scharlau Chemicals), 152 NaCl, 1 MgCl2, 10 HEPES (all from VWR chemicals), 10 glucose (MP Biomedicals) and 2 CaCl2 (Merck KGaA) at pH 7.4 (all mM). Fluorescence was visualized using the imaging setup (TILL Photonics GmbH) consisting of a monochromatic light source and a CCD camera (SensiCam) with ex 495 nm, em ≥520 nm, exposure time 100 ms and binning 2. The baseline was measured for 2 min before applying either 100 µM ATP or ADP (both Sigma) for 5 s, followed with 2 min stabilization, and application of 10 µM ionomycin (Tocris Bioscience) for 2s to induce maximal response. The chemicals were applied using a fast perfusion system Rapid Solution Changer RSC-200 (BioLogic Science). For quantification, the baseline was subtracted and the maximum amplitudes evoked by ATP or ADP were divided by the maximum amplitude of ionomycin to get a ratio. Data were analyzed using FEI offline analysis (TILL Photonics) and ImageJ (U. S. National Institutes of Health) and further analysis was automatized using MatLab (The MathWorks, Inc) and Origin (OriginLab Corporation).

Migration assay
IncuCyte® scratch wound cell migration assay (Sartorius) was performed according to manufacturer's instructions through real-time visualization. In brief, confluent monolayer of iMGLs on PDL-coated 96-well ImageLock™ microplates (EssenBioScience) was wounded using a 96-well WoundMaker to create homogeneous, 700-800µm wide wounds and the cells were treated with 100 µM ATP, ADP, or CX3CL1 (Peprotech), or freshly reconstituted 1 µM sAβ (Bachem). Live-cell imaging scans in bright field were repeated every hour for 24 h. The wound width, confluence and relative wound density were analyzed with IncuCyte S3 2018 software (Essen BioScience).

Phagocytosis assays
pHrodo™ Zymosan A BioParticle phagocytosis assay (Thermo Fisher Scientific) was performed using IncuCyte live cell imaging. iMGLs were prestimulated for 24 h with 100 ng/ml LPS (Sigma), 20 ng/ml IFNγ (Peprotech) or LPS-IFNγ (100ng/ml, 20 ng/ml) or were treated with 1µM sAβ or insoluble fAβ Aβ1-42 at the time of bead application in microglial maturation medium without FBS on PDL-coated nunc 96-well plates. fAβ was prepared from sAβ by incubating at 37°C for 7 days. pHrodo bioparticles were added in Opti-MEM (Gibco) at 62.5µg/ml and cells live-cell imaged in IncuCyte S3 every 30 minutes for 6 h to obtain fluorescent-time curve. Additionally, nuclei were stained after 2 h bead incubation with 5 µg/ml H33342 for 5 min and iMGLs were live-imaged using a ZEISS IX70 fluorescent microscope with Axio Observer.Z1 (ZEISS) with 20X magnification. The total pHrodo fluorescence intensity was normalized to cell confluence analyzed by IncuCyte S3 2018 or to number of nuclei analyzed by ImageJ. In addition, FITC Zymosan A S. cerevisiae BioParticles (Thermo Fisher Scientific) were opsonized in FBS and added on iMGLs on Matrigel-coated glass coverslips at density of 1.5 bioparticles per cell. The assay was terminated by 4% PFA fixation after 2.5-3 h. Coverslips were washed 8x for 5 min using TBS to remove free beads that had not been internalized. Nuclei were stained using 1 µg/mL Hoechst 33342 (Thermo Fisher Scientific). Coverslips were mounted on glass microscope slides using Prolong Gold Antifade reagent (Thermo Fisher Scientific) and were imaged using a Leica SP8 confocal microscope (Leica). For quantification, fluorescence was measured as corrected mean grey value and analyzed using ImageJ.

Cytometric Bead Array
Cytokine secretion iMGLs was analyzed using the Cytometric Bead Array (CBA) with human soluble protein flex sets (all from BD Biosciences). The medium was collected from plates prestimulated for 24h for pHrodo assays. Media was diluted 1:1 for LPS-treated and 1:10 for LPS-IFNγ-treated samples in assay diluent. Twenty microliters of sample or cytokine standard was incubated with 20 µl of bead mixture (bead dilutions 1:75) and then with 20ul of diluted detection reagent (1:75). Samples run on Cytoflex S (Beckman Coulter) by detecting at least 300 events for each cytokine. Beads positions clustered with channels 638/660 nm (APC) and 638/780 nm (APC-A750) off the 638 nm red laser. Cytokine reporter PE fluorescence was measured through 561/585 nm channel off 561 nm yellow-green laser. The data was analyzed with FCAP array (SoftFlow) and regression analysis was used to calculate cytokine concentrations from known standards.

MitoStress mitochondrial metabolism assay

Mitochondrial metabolism of iMGLs was analyzed with MitoStress test (Agilent) following manufacturer's guidelines. The cells were pre-stimulated for 24 h with LPS, IL-4 (Peprotech), IFNγ or with LPS-IFNγ (20 ng/ml for all) at density of 150 000 cells/well. The XF assay medium (Agilent) was supplemented with 25 mM GlutaMAX and 1 mM sodium pyruvate (Gibco). Mitochondrial electron transport chain modulators all 1 µM were injected during the assay sequentially: 1) oligomycin to inhibit ATP synthase, 2) carbonyl cyanide-4-(trifluoromethoxy)phenylhydrazone (FCCP) to disrupt the proton gradient and membrane potential, and 3) a mixture of rotenone and antimycin A (RA) to switch off the mitochondrial respiration (all from Sigma). Changes in OCR in response to injections were detected with Seahorse XF24 analyzer (Agilent). Results were normalized to total protein content measured with Pierce BCA protein assay kit and the data was analyzed with Wave 2.4 (Agilent). Mitochondrial parameters were calculated from OCRs according to manufacturer's instructions.

Experimental Procedures References

Aibar, S., Gonzalez-Blas, C.B., Moerman, T., Huynh-Thu, V.A., Imrichova, H., Hulselmans, G., Rambow, F., Marine, J.C., Geurts, P., Aerts, J., et al 2017, "SCENIC: single-cell regulatory network inference and clustering", *Nature methods*, vol. 14, no. 11, pp. 1083-1086.

Bolstad, B.M., Irizarry, R.A., Astrand, M. & Speed, T.P. 2003, "A comparison of normalization methods for high density oligonucleotide array data based on variance and bias", *Bioinformatics (Oxford, England)*, vol. 19, no. 2, pp. 185-193.

Choi, S.H., Kim, Y.H., Hebisch, M., Sliwinski, C., Lee, S., D'Avanzo, C., Chen, H., Hooli, B., Asselin, C., Muffat, J., et al 2014, "A three-dimensional human neural cell culture model of Alzheimer's disease", *Nature*, vol. 515, no. 7526, pp. 274-278.

Colella, S., Yau, C., Taylor, J.M., Mirza, G., Butler, H., Clouston, P., Bassett, A.S., Seller, A., Holmes, C.C. & Ragoussis, J. 2007, "QuantiSNP: an Objective Bayes Hidden-Markov Model to detect and accurately map copy number variation using SNP genotyping data", *Nucleic acids research*, vol. 35, no. 6, pp. 2013-2025.

Kim, Y.H., Choi, S.H., D'Avanzo, C., Hebisch, M., Sliwinski, C., Bylykbashi, E., Washicosky, K.J., Klee, J.B., Brustle, O., Tanzi, R.E., et al 2015, "A 3D human neural cell culture system for modeling Alzheimer's disease", *Nature protocols*, vol. 10, no. 7, pp. 985-1006.

Lancaster, M.A. & Knoblich, J.A. 2014, "Generation of cerebral organoids from human pluripotent stem cells", *Nature protocols*, vol. 9, no. 10, pp. 2329-2340.

Li, B. & Dewey, C.N. 2011, "RSEM: accurate transcript quantification from RNA-Seq data with or without a reference genome", *BMC bioinformatics*, vol. 12, pp. 323-2105-12-323.

Lim, S.Y., Sivakumaran, P., Crombie, D.E., Dusting, G.J., Pebay, A. & Dilley, R.J. 2013, "Trichostatin A enhances differentiation of human induced pluripotent stem cells to cardiogenic cells for cardiac tissue engineering", *Stem cells translational medicine*, vol. 2, no. 9, pp. 715-725.

Love, M.I., Huber, W. & Anders, S. 2014, "Moderated estimation of fold change and dispersion for RNA-seq data with DESeq2", *Genome biology*, vol. 15, no. 12, pp. 550-014-0550-8.

Ritchie, M.E., Phipson, B., Wu, D., Hu, Y., Law, C.W., Shi, W. & Smyth, G.K. 2015, "limma powers differential expression analyses for RNA-sequencing and microarray studies", *Nucleic acids research*, vol. 43, no. 7, pp. e47.

Ruijter, J.M., Ramakers, C., Hoogaars, W.M., Karlen, Y., Bakker, O., van den Hoff, M.J. & Moorman, A.F. 2009, "Amplification efficiency: linking baseline and bias in the analysis of quantitative PCR data", *Nucleic acids research*, vol. 37, no. 6, pp. e45.

Schmittgen, T.D. & Livak, K.J. 2008, "Analyzing real-time PCR data by the comparative C(T) method", *Nature protocols*, vol. 3, no. 6, pp. 1101-1108.

Soneson, C., Love, M.I. & Robinson, M.D. 2015, "Differential analyses for RNA-seq: transcript-level estimates improve gene-level inferences", *F1000Research*, vol. 4, pp. 1521.

Viswanathan, J., Haapasalo, A., Bottcher, C., Miettinen, R., Kurkinen, K.M., Lu, A., Thomas, A., Maynard, C.J., Romano, D., Hyman, B.T., et al 2011, "Alzheimer's disease-associated ubiquilin-1 regulates presenilin-1 accumulation and aggresome formation", *Traffic (Copenhagen, Denmark)*, vol. 12, no. 3, pp. 330-348.

Wang, K., Li, M., Hadley, D., Liu, R., Glessner, J., Grant, S.F., Hakonarson, H. & Bucan, M. 2007, "PennCNV: an integrated hidden Markov model designed for high-resolution copy number variation detection in whole-genome SNP genotyping data", *Genome research*, vol. 17, no. 11, pp. 1665-1674.

Wheeler, D.L., Barrett, T., Benson, D.A., Bryant, S.H., Canese, K., Chetvernin, V., Church, D.M., DiCuccio, M., Edgar, R., Federhen, S., et al 2007, "Database resources of the National Center for Biotechnology Information", *Nucleic acids research*, vol. 35, no. Database issue, pp. D5-12.